Nonlinear Dynamics and Neuroscience

Izvestiya Vysshikh Uchebnykh Zavedeniy. Applied Nonlinear Dynamics. 2024;32(3)

Article DOI: 10.18500/0869-6632-003113

Synchronization regimes in the ring of rodent hippocampal neurons at limbic epilepsy

M. V. Kornilov[1,2]✉, *A. A. Kapustnikov*[1,2], *E. A. Sozonov*[2], *M. V. Sysoeva*[1], *I. V. Sysoev*[1,2]

[1]Saratov Branch of Kotelnikov Institute of Radioengineering and Electronics, Russia
[2]Saratov State University, Russia
E-mail: ✉kornilovmv@gmail.com, anton.kapustnikov.02@mail.ru, infagot@gmail.com, bobrichek@mail.ru, ivssci@gmail.com

Received 19.11.2023, accepted 18.02.2024, available online 7.05.2024, published 31.05.2024

Abstract. This study *aims* to consider an ensemble of hippocampal neurons coupled in a ring, which may be responsible for generation of the primary rhythm at limbic epilepsy. *Methods.* Model equations were solved numerically. To determine the areas of oscillatory and excitable regime existance for a single neuron, the bifurcation analysis for the leakadge conductivity parameter was performed. The coupling delays was not implemented directly, instead, inertia in the synapse was introduced. To determine the stability of generation some couplings were removed and parameter detunig was introduced. *Results.* In the single neuron model the bistability region was detected, in which a stable focus coexhists with a limit cycle. Two main synchronous regimes were detected. The first regime inherits frequency of individual oscillator, with a relatively small phase shift between oscillators in the ring. The frequency of the second regime depends on the number of neurons in the ring, with the phase shift between neighbor oscillators being equal to ratio of oscillation period and number of neurons. This second regime can occur both for the parameters corresponding to bistabler regime in the individual neuron and for the parameters at which the only existing attractor is stable focus. The second synchronous regime is preserved for parameter detuning of 2% from their absolute values. *Conclusion.* It was shown that in the mathematical model of the ring of hippocampal neurons, where all the main significant currents are taken into account for individual neurons, and their parameters can vary, there is an oscillatory mode, the frequency of which is determined by the length of the ring and synaptic conductivity, rather than by the parameters individual neuron. In this case, a small change in synaptic conductivity can lead to a sharp (2–7 times) change in the generation frequency.

Keywords: Hodgkin–Huxley model, neural networks, collective dynamics, hippocampus, pyramidal neuron, epilepsy.

Acknowledgements. This study was supported by Russian Science Foundation, grant No. 19-72-10030-П, https://rscf.ru/project/19-72-10030/.

For citation: Kornilov MV, Kapustnikov AA, Sozonov EA, Sysoeva MV, Sysoev IV. Synchronization regimes in the ring of rodent hippocampal neurons at limbic epilepsy. Izvestiya VUZ. Applied Nonlinear Dynamics. 2024;32(3):357–375. DOI: 10.18500/0869-6632-003113

Introduction

Epilepsy is a complex of various types of functional disorders that lead to disruptions in the normal functioning of the brain. The common place of all forms of epilepsy is the generation of relatively synchronous, high-amplitude pathological electromagnetic activity by neurons of one or more brain systems, for example, thalamocortical or limbic system. Different forms of epilepsy have different etiology (origin) and differ both by the areas involved in the generation of pathological activity and by the scenario of the occurrence and development of epileptic activity. In this regard, modeling different types of epilepsy from the point of view of the theory of dynamical systems must be made differently, and the description of epileptic activity in a particular form can be achieved by involving specific concepts. Thus, for modeling absence epilepsy, the structure of connections in the thalamocortical network is important, while the thalamus and cortex cannot be considered in isolation since oscillations appear immediately throughout the system. Spike-wave discharges in absence epilepsy are highly nonlinear oscillations with a specific shape and spectrum that persist throughout the discharge. Therefore, a large number of works were devoted mainly to reproducing these features [2]. It is important that the processes in the brain responsible for the cessation of pathological activity have not yet been discovered, which led to the creation of a number of models of spike-wave discharges based on the concept of transients [3, 4] in contrast to earlier models based on switching between attractors, one of which responsible for normal, and the second — for epileptiform activity [2,5]. At the same time, in limbic epilepsy, pathological activity is initially and for a long time concentrated inside the hippocampus, and the question of how the basic rhythm is formed and evolves is important, since the frequency and shape of oscillations change greatly during discharge and may even differ qualitatively in different subjects [6]. At the same time, the spread of pathological activity beyond the primary network of the hippocampus (secondary generalization) is a separate process that can occur months and years after the formation of the primary generator of pathological activity and has its own mechanisms [7].

In the work [8] it was shown that the generator of epileptiform activity can be implemented in the form of a ring of neurons, each of those is in a subthreshold non-oscillatory mode, and the final activity is a function of connections and delay time in the synapse: an impulse excited by an external input (another neuron not included in the oscillatory ring) sequentially runs through to all cells of the ring and again excites the first neuron, etc. The model proposed in [8] had a number of disadvantages, namely:

- The Hodgkin-Huxley equations in their original form were used to describe an individual neuron, while hippocampal cells have significant specificity and are described by more complex models with a large number of equations, other parameter values and excellent nonlinear functions [9];
- the delay was added to the communication function directly for simplicity, while in reality the delay is a function of synapse inertia;
- all the neurons in the ring were identical in parameters.

Considering the delay as a delay line in a electronic generator made it possible in the works of [8, 10] to investigate a large set of modes and obtain an analytical dependence of the generation frequency on the delay and delay time. But if we talk about the initial biological system, it is important to understand the limits within which the delay can change are important for understanding what frequencies can be achieved. The identity of the neurons in the ring obviously contributes to the synchronization of oscillations with a lag equal (in the considered cases) to T/D, where T is the oscillation period, and D is the number of oscillators in the ring. But in a real system, all neurons will be different, and it is important to know how stable the studied regime will be. Thus, the solution of all these issues is necessary to confirm the

fundamental possibility of the existence of the modes found in [8, 10] in hippocampal networks, which is what this work is devoted to.

1. Model

1.1. Node Model. A single-compartment (single-chamber) Hodgkin-Huxley [11] model was used as a network node, written in accordance with [12,13] for pyramid cells of the hippocampal CA3 field (1). It should be noted that when writing equations, there are two main approaches to the dimensionality of the capacitance and conductivity parameters. The first approach is as follows: parameter values are written for the entire neuron as if it were a localized in space element (we can also assume that the parameters correspond to the result of integration over the area of the entire neuron). The second approach is to record the specific conductivities and capacitances per unit area [9], which can be useful, for example, when switching from single-compartment to multi-compartment models. In this paper, we used integrated values, since the values were taken from the work [13].

$$C\frac{dV_i}{dt} = -I_{\mathrm{Na}i} - I_{\mathrm{Ca}i} - I_{\mathrm{Ca(low)}_i} - I_{\mathrm{K(DR)}_i} - I_{\mathrm{K(A)}_i} - I_{\mathrm{K(AHP)}_i} - I_{\mathrm{K(C)}_i} - I_{\mathrm{L}i} - I_{\mathrm{syn}_i}, \qquad (1)$$

where V_i is the potential on the membrane of the i-th neuron, t is the dimensional time, C is the membrane capacity (in this work $C = 0.1\mu\mathrm{F}$). The currents of the ion channels are described below.

I_{Na} is a *sodium current*:

$$\begin{aligned} I_{\mathrm{Na}i} &= g_{\mathrm{Na}i} m_i^2 h_i (V_i - V_{\mathrm{Na}i}), \\ \frac{dm_i}{dt} &= \alpha_{\mathrm{m}}(V_i)(1 - m_i) - \beta_{\mathrm{m}}(V_i) m_i, \\ \frac{dh_i}{dt} &= \alpha_{\mathrm{h}}(V_i)(1 - h_i) - \beta_{\mathrm{h}}(V_i) h_i, \end{aligned}$$

where the maximum electrical conductivity of the sodium channel is $\overline{g}_{\mathrm{Na}} = 1.0\ \mu\mathrm{S}$, the equilibrium potential (reversal potential) of the sodium channel is $\overline{V}_{\mathrm{Na}} = 50.0$ mV. For $\overline{g}_{\mathrm{Na}}$ and $\overline{V}_{\mathrm{Na}}$, the average values are indicated, since later in the work, among other things, an experiment with detuning according to these parameters is described. m, h are gate variables of the sodium channel, α and β are functions of opening and closing gate variables (transitions):

$$\alpha_{\mathrm{m}}(V_i) = \frac{-0.32(V_i + 51.9)}{\exp(-(V_i + 51.9)/4) - 1}, \quad \beta_{\mathrm{m}}(V_i) = \frac{0.28(V_i + 24.9)}{\exp((V_i + 24.9)/5) - 1},$$

$$\alpha_{\mathrm{h}}(V_i) = 0.128\exp(-(V_i + 48)/18), \quad \beta_{\mathrm{h}}(V_i) = \frac{4}{1 + \exp(-(V_i + 25)/5)}.$$

I_{Ca} is a *calcium current*:

$$\begin{aligned} I_{\mathrm{Ca}i} &= g_{\mathrm{Ca}i} s_i^2 r_i (V_i - V_{\mathrm{Ca}i}), \\ \frac{ds_i}{dt} &= \alpha_{\mathrm{s}}(V_i)(1 - s_i) - \beta_{\mathrm{s}}(V_i) s_i, \\ \frac{dr_i}{dt} &= \alpha_{\mathrm{r}}(V_i)(1 - r_i) - \beta_{\mathrm{r}}(V_i) r_i, \end{aligned}$$

where $\overline{g}_{\mathrm{Ca}} = 0.13\ \mu\mathrm{S}$, $\overline{V}_{\mathrm{Ca}} = 75.0$ mV, s, r — gate variables of the sodium channel, transition functions:

$$\alpha_{\mathrm{s}}(V_i) = \frac{0.2}{1+\exp(-0.072V_i)}, \qquad \beta_{\mathrm{s}}(V_i) = \frac{0.0025(V_i+13.9)}{\exp((V_i+13.9)/5)-1},$$

$$\alpha_{\mathrm{r}}(V_i) = \begin{cases} \dfrac{\exp(-(V_i+65)/20)}{1600} & (V_i > -65), \\ 0.000625 & (V_i \leqslant -65), \end{cases}$$

$$\beta_{\mathrm{r}}(V_i) = \begin{cases} \dfrac{0.005 - 8\alpha_{\mathrm{r}}(V_i)}{8} & (V_i > -65), \\ 0 & (V_i \leqslant -65), \end{cases}$$

$I_{\mathrm{Ca(low)}}$ is a *low-threshold calcium current*:

$$\begin{aligned} I_{\mathrm{Ca(low)}_i} &= g_{\mathrm{Ca(low)}_i} s^2_{\mathrm{Ca(low)}_i} r_{\mathrm{Ca(low)}_i}(V_i - V_{\mathrm{Ca}i}), \\ \frac{ds_{\mathrm{Ca(low)}_i}}{dt} &= \alpha_{\mathrm{s}_{\mathrm{Ca(low)}}}(V_i)\left(1 - s_{\mathrm{Ca(low)}_i}\right) - \beta_{\mathrm{s}_{\mathrm{Ca(low)}}}(V_i) s_{\mathrm{Ca(low)}_i}, \\ \frac{dr_{\mathrm{Ca(low)}_i}}{dt} &= \alpha_{\mathrm{r}_{\mathrm{Ca(low)}}}(V_i)\left(1 - r_{\mathrm{Ca(low)}_i}\right) - \beta_{\mathrm{r}_{\mathrm{Ca(low)}}}(V_i) r_{\mathrm{Ca(low)}_i}, \end{aligned}$$

where $\overline{g}_{\mathrm{Ca(low)}} = 0.03$ μS, $\overline{V}_{\mathrm{Ca}} = 75.0$ mV, $s_{\mathrm{Ca(low)}}, r_{\mathrm{Ca(low)}}$ are gate variables, functions transitions:

$$\alpha_{\mathrm{s}_{\mathrm{Ca(low)}}}(V_i) = \frac{1.6}{1+\exp(-0.072(V_i+40))}, \quad \beta_{\mathrm{s}_{\mathrm{Ca(low)}}}(V_i) = \frac{0.02(V_i+53.9)}{\exp((V_i+53.9)/5)-1},$$

$$\alpha_{\mathrm{r}_{\mathrm{Ca(low)}}}(V_i) = \begin{cases} \dfrac{\exp(-(V_i+105)/20)}{200}, & (V_i > -105) \\ 0.005, & (V_i \leqslant -105) \end{cases}$$

$$\beta_{\mathrm{r}_{\mathrm{Ca(low)}}}(V_i) = \begin{cases} 0.005 - \alpha_{\mathrm{r}_{\mathrm{Ca(low)}}}(V_i), & (V_i > -105) \\ 0, & (V_i \leqslant -105) \end{cases}$$

$I_{\mathrm{K(DR)}}$ is a *fast delayed rectification potassium current*:

$$\begin{aligned} I_{\mathrm{K(DR)}_i} &= g_{\mathrm{K(DR)}_i} n_i (V_i - V_{\mathrm{K}i}), \\ \frac{dn_i}{dt} &= \alpha_{\mathrm{n}}(V_i)(1-n_i) - \beta_{\mathrm{n}}(V_i) n_i, \end{aligned}$$

where $\overline{g}_{\mathrm{K(DR)}} = 0.08$ μS, $\overline{V}_{\mathrm{K}} = -80$mV, n is gate variable (transition constants):

$$\alpha_{\mathrm{n}}(V_i) = \frac{-0.016(V_i+29.9)}{\exp(-(V_i+29.9)/5)-1}, \quad \beta_{\mathrm{n}}(V_i) = 0.25\exp(-(V_i+45)/40).$$

$I_{\mathrm{K(A)}}$ is an *A-type potassium current*:

$$\begin{aligned} I_{\mathrm{K(A)}_i} &= g_{\mathrm{K(A)}_i} a_i b_i (V_i - V_{\mathrm{K}i}), \\ \frac{da_i}{dt} &= \alpha_{\mathrm{a}}(V_i)(1-a_i) - \beta_{\mathrm{a}}(V_i) a_i, \\ \frac{db_i}{dt} &= \alpha_{\mathrm{b}}(V_i)(1-b_i) - \beta_{\mathrm{b}}(V_i) b_i, \end{aligned}$$

where $\overline{g}_{\mathrm{K(A)}} = 0.17$ μS, $\overline{V}_{\mathrm{K}} = -80$ mV, a, b are gate variables (transition constants):

$$\alpha_{\mathrm{a}}(V_i) = \frac{-0.02(V_i + 51.9)}{\exp(-(V_i + 51.9)/10) - 1}, \quad \beta_{\mathrm{a}}(V_i) = \frac{0.0175(V_i + 24.9)}{\exp((V_i + 24.9)/10) - 1},$$

$$\alpha_{\mathrm{b}}(V_i) = 0.0016\exp(-(V_i + 78)/18), \quad \beta_{\mathrm{b}}(V_i) = \frac{0.05}{1 + \exp(-(V_i + 54.9)/5)}.$$

$I_{\mathrm{K(AHP)}}$ is a *slow calcium-dependent potassium current after hyperpolarization*:

$$\begin{aligned} I_{\mathrm{K(AHP)}_i} &= g_{\mathrm{K(AHP)}_i} q_i (V_i - V_{\mathrm{K}i}), \\ \frac{dq_i}{dt} &= \alpha_{\mathrm{q}}(V_i)(1 - q_i) - \beta_{\mathrm{q}}(V_i) q_i, \end{aligned}$$

where $\overline{g}_{\mathrm{K(HP)}} = 0.07$ μS, $\overline{V}_{\mathrm{K}} = -80$ mV, q is a gate variable, transition functions:

$$\alpha_{\mathrm{q}}(V_i) = \begin{cases} 0, & ((\chi_i - 140) < 0) \\ 0.00002(\chi_i - 140), & (0 \leqslant (\chi_i - 140) < 500) \\ 0.01, & (500 \leqslant (\chi_i - 140)) \end{cases}$$

$$\beta_{\mathrm{q}}(V_i) = 0.001.$$

$I_{\mathrm{K(C)}}$ is a *fast calcium-dependent potassium current*:

$$\begin{aligned} I_{\mathrm{K(C)}i} &= g_{\mathrm{K(C)}_i} \min(1, \chi_i/250) c_i (V_i - V_{\mathrm{K}i}), \\ \frac{dc_i}{dt} &= \alpha_{\mathrm{c}}(V_i)(1 - c_i) - \beta_{\mathrm{c}}(V_i) c_i, \\ \frac{d\chi_i}{dt} &= -\phi I_{\mathrm{Ca}i} - \beta_\chi \chi_i, \end{aligned}$$

where $\overline{g}_{\mathrm{K(C)}} = 0.366$ μS, $\overline{V}_{\mathrm{K}} = -80$mV, $\phi = 50\mathrm{ms}^{-1}$, $\beta_\chi = 0.075\mathrm{ms}^{-1}$, c, χ are gate variables (transition constants):

$$\alpha_{\mathrm{c}}(V_i) = \begin{cases} \dfrac{1}{18.975} \exp(((V_i + 55)/11) - ((V_i + 58.5)/27)) & (V_i \leqslant -15), \\ 2\exp(-(V_i + 58.5)/27) & (V_i > -15), \end{cases}$$

$$\beta_{\mathrm{c}}(V_i) = \begin{cases} 2\exp(-(V_i + 58.5)/27) - \alpha_{\mathrm{c}}(V_i) & (V_i \leqslant -15), \\ 0 & (V_i > -15), \end{cases}$$

I_{L} is a *leakage current*:

$$I_{\mathrm{L}i} = g_{\mathrm{L}i}(V_i - V_{\mathrm{L}i}),$$

where the leakage conductivity $\overline{g}_{\mathrm{L}}$ varied depending on the position of the neuron in the network, the equilibrium leakage potential $\overline{V_L} = -65$ mV.

I_{syn} is a *synaptic current*:

$$I_{\mathrm{syn}_i} = \quad g_{\mathrm{syn}_i}(V_i - V_{\mathrm{syn}_i}) \sum p_j, \tag{2}$$

where the conductivity of the excitatory synapse $\overline{g}_{\text{syn}}$ changed during the experiments, the equilibrium potential of the excitatory synapse $\overline{V}_{\text{syn}} = 0$ mV, p_j are gate variables related to presynaptic neurons:

$$\frac{dp_j}{dt} = \alpha_{\text{p}} \frac{(1 - p_j)}{1 + \exp(-(V_j - 2)/5)} - \beta_{\text{p}} p_j, \tag{3}$$

transition constants $\alpha_{\text{p}} = 1.1$ ms^{-1} and $\beta_{\text{p}} = 0.19$ ms^{-1}, V_j is presynaptic neuron potential.

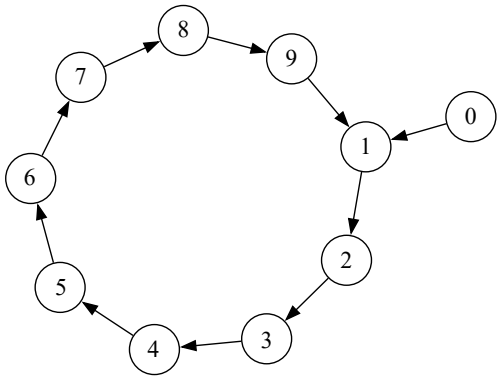

Fig 1. The structure of the considered network of hippocampal neurons. Neuron No.0 is used only to trigger oscillatory activity and is not directly involved in rhythm generation

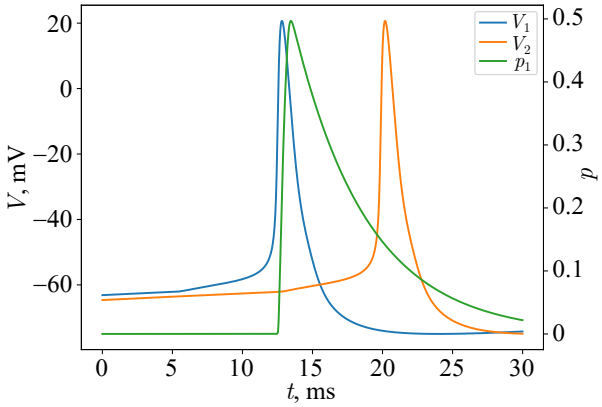

Fig 2. Synapse inertia. The blue line shows the change in the value of the potential on the presynaptic neuron membrane on time $V_1(t)$. The green line shows the dependence of the gate variable of the presynaptic neuron on time $p(t)$. The orange line shows the change in the value of the potential on the postsynaptic neuron membrane on time $V_2(t)$, $\overline{g}_{\text{syn}} = 2.5{\cdot}10^{-3}$ μS, $w = 100$ ms (color online)

1.2. Network model. The neurons were closed in a ring, connected by a unidirectional excitatory synapse (Fig. 1). The number of elements varied from 2 to 35. The parameters of the ring neurons were set in such a way that a single element was in a non-oscillatory subthreshold mode. The starting neuron No. 0 was in an oscillatory mode. A short-term impact was applied from the starting neuron No. 0 to the ring neuron No. 1 (the duration of the impact w varied in the range $[100; 500]$ ms).

The mathematical model of the synapse (2, 3) was taken from [9]. Unlike previously published works [8, 10] no additional time delay was introduced into the synapse formula. Instead, the self inertia parameter of the model was used. Fig. 2 shows the time realizations of the potential V_1 on the membrane the first neuron in the ring and the values of the gate variable p of the same neuron (it is proportional to the potential on the axon of this neuron), as well as the potential V_2 on the membrane of the next neuron in ring. One oscillation is shown after skipping 6 s from the beginning of the experiment, that is, after skipping all transient processes and establishing an oscillatory regime in the ring. The results are given at a synaptic conductivity value of $\overline{g}_{\text{syn}} = 2.5 \cdot 10^{-3}$μS. The study of signal transmission through the synapse at other values of $\overline{g}_{\text{syn}}$ made it possible to determine that the greater is the value of synaptic conductivity, the less is the delay between the time series of two neighbor neurons.

Here and below, the system of equations for both an individual neuron and a ring was solved by the Runge–Kutta method of order 5(4), in which steps are taken in accordance with the 5-th order formula, but the error is controlled by the 4-th order of accuracy. For this purpose, the implementation from the `scipy.integrate` [14] package was used. A comparison with the results of integrating a system of equations using the

Adams method of 8-th order of accuracy showed minor differences in the length of the transient process that do not affect the characteristics of the steady state.

2. Results

2.1. Dynamics of an isolated neuron. To detect the existence limits of oscillatory and excitable modes, a partial bifurcation analysis of the model was carried out using the leakage conductivity parameter g_{L}, since this parameter is the most clearly responsible for losses in the system. For this purpose, the dependence of the frequency and amplitude of oscillations on the leakage conductivity g_{L} was plotted for one isolated neuron (Fig. 3) at two different initial conditions for the variable V: close to the equilibrium potential $V(t = 0) = -62$ mV and caused by an external pulse $V(t = 0) = 20$ mV. The initial conditions for all other variables were set to correspond to the stable equilibrium position observed at $g_{\mathrm{L}} = 0.040$μS. From Fig. 3, *b* it is clear that on the segment $g_{\mathrm{L}} \in [0.0376; 0.0404]$μS there is bistability: a stable point, reached at $V(t = 0) = -62$ mV, coexists with an oscillatory mode, which can be obtained at $V(t = 0) = 20$ mV. In this case, the oscillatory mode itself is the heir (the amplitude and frequency change continuously as g_{L} decreases) of the oscillatory mode that exists at lower values of g_{L}. This situation can be explained by the fact that at $0.0374 < g_{\mathrm{L}} < 0.0376$ a subcritical Andronov–Hopf bifurcation occurs, as a result of which an unstable cycle is born from an unstable focus, and the focus becomes stable. Further, at $g_{\mathrm{L}} \approx 0.0406$, the stable cycle disappears, and its amplitude before this is finite, which can be explained by its merger with the unstable cycle.

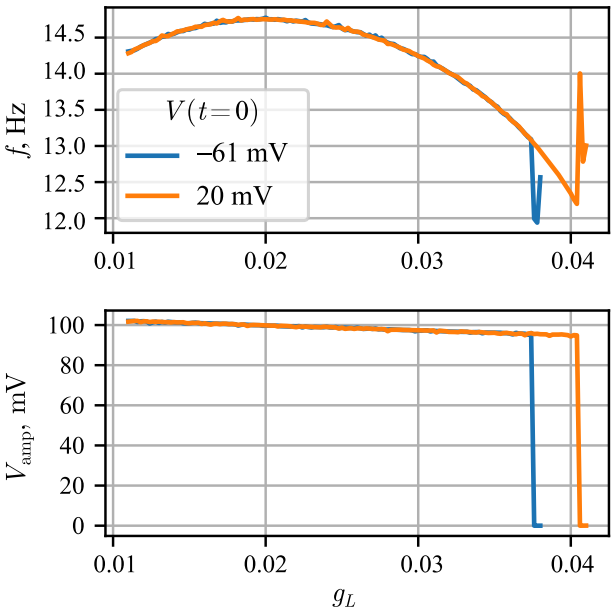

Fig 3. The dependence of the main oscillation frequency and amplitude with a change in the leakage conductivity g_{L} for one uncoupled node (color online)

In the previously published works [8, 10] generation in a ring was always considered with the parameters of an individual neuron corresponding to the excitable mode (stable focus). But the presence of bistability on the interval $g_{\mathrm{L}} \in [0.0376; 0.0404]$ μS prompted us to consider the system at two different g_{L}: 0.040 μS and 0.043 μS, to determine how much a limit cycle coexisting with a stable focus could distort the dynamics in the ring.

2.2. A network of homogeneous elements. First, we considered a network consisting of identical neurons i. e. without parameter detuning. The model equations were solved for different values of synapse conductivity $\overline{g}_{\mathrm{syn}}$, which in some way can be considered as an analogue of the coupling coefficient between network elements k from the work [8]. The $\overline{g}_{\mathrm{syn}}$ parameter varied in the range $[2 \cdot 10^{-3}; 4 \cdot 10^{-3}]$ μS.

Fig. 4, *a* shows the dependence of the oscillation frequency in the f ring on the number of neurons in the D network for different values of synaptic conductivity $\overline{g}_{\mathrm{syn}}$ for leakage conductivity $g_{\mathrm{L}} = 0.040$μS. At small D, a quasi-synchronous mode is observed (see Fig. 5, *a*), the frequency of

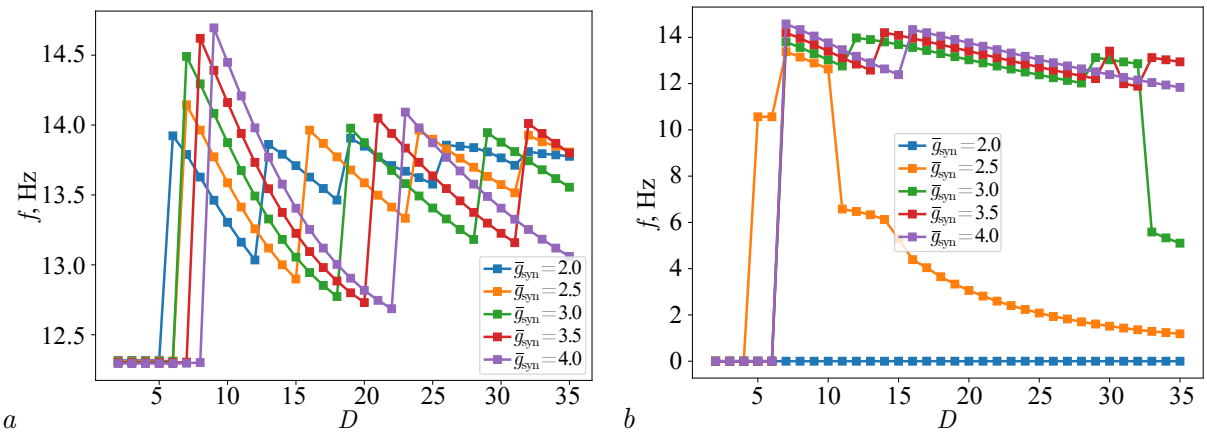

Fig 4. The dependence of the oscillation frequency in the ring f on the number of neurons in the network D at different values of synaptic conductivity $\overline{g}_{\text{syn}}$. w = 100 ms. Leakage conductivity: a — $\overline{g}_{\text{L}} = 0.040$ μS, b — $\overline{g}_{\text{L}} = 0.043$ μS (color online)

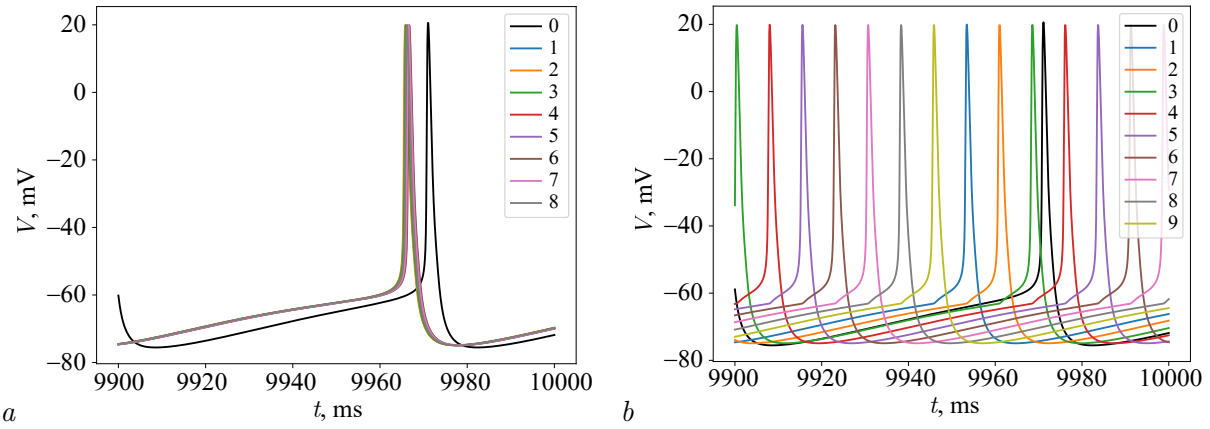

Fig 5. Time series at $\overline{g}_{\text{syn}} = 4.0 \cdot 10^{-3}$ μS, w = 100 ms. a — the number of neurons in the ring $D = 8$. b — the number of neurons in the ring $D = 9$ (color online)

which does not depend on the number of neurons in the network and on the coupling strength. This mode is a direct descendant of the cycle in a separate neuron, coexisting with a stable focus; it has the same frequency and amplitude. The observed time lag between neurons in the ring is due to the finite inertia of the synapse. The neurons in the formed train seem to line up one after another, with the neuron that received the exciting impulse coming ahead in time, and then all the others in order in a ring with a small time lag. The quasi-synchronous regime, close to the full synchronization regime, is destroyed as D increases. The smaller the synaptic conductivity of $\overline{g}_{\text{syn}}$ is, the smaller the area of its existence becomes: for $\overline{g}_{\text{syn}} = 2$ it disappears already at $D = 6$, while for $\overline{g}_{\text{syn}} = 4$ — only at $D = 9$. This observation naturally agrees with the general theory [15], since synaptic conductivity in the considered model plays the role of coupling strength.

At large values of D, a family of regimes is observed that are qualitatively similar to the regimes observed in the works [8, 10] (see Fig. 5, b). In them, all oscillators are shifted in phase one relative to the other at equal intervals in such a way that the total shift along the ring is

2π; so the sum of all time shifts is equal to the oscillation period. The frequency of oscillations decreases as the number of oscillators increases. However, such modes are stable only in a narrow frequency range. It can be seen that, first, as the number of neurons increases, the frequency decreases nonlinearly (the curve for $\overline{g}_{\text{syn}} = 4$ is close to a hyperbola), then it increases sharply and at finally begins to fall again. Moreover, the smaller $\overline{g}_{\text{syn}}$ is (i. e. the closer the neurons are to the oscillatory mode), the more often (along the X-axis) jumps occur. Previously, jumps in the dependence $f(D)$ were observed in a ring of FitzHugh–Nagumo neurons in the work [10], but there the increase in frequency was more significant: during the first jump it rose approximately twice, which corresponded to the regime when two pulses propagate simultaneously in antiphase along the ring. In this system, there is only one impulse left.

For leakage conductivity $\overline{g}_{\text{L}} = 0.043$ μS, at which the cycle for an individual neuron has already collapsed, the dependences $f(D)$ have significant differences. For $\overline{g}_{\text{syn}} = 2$ oscillations are not excited at all. It is likely that the connectivity strength in the ring is not sufficient to compensate for the attenuation. At $\overline{g}_{\text{syn}} \geqslant 3$, regimes are observed that are qualitatively similar to what occurred at $\overline{g}_{\text{L}} = 0.04$ μS; there are also frequency jumps. The most interesting dynamics is observed at $\overline{g}_{\text{syn}} = 2.5$, starting from $D \geqslant 11$. When switching from $D = 10$ to $D = 11$, the frequency drops sharply from 12.5 Hz to 6.5 Hz and it continues to decrease further with increasing D to less than 2 Hz at $D > 25$. Similar dynamics of $f(D)$ is observed for $\overline{g}_{\text{syn}} = 3$, but with a very large number of neurons in the ring: starting from $D = 33$. Thus, a relatively small decrease in the synaptic conductivity between values of 3 and 2 μS can lead first to a sharp drop in the generation frequency, and then — to the oscillation death. This is precisely the behavior that was previously recorded in some neurophysiological experiments. [16, 17].

2.3. System stability to perturbations of connectivity matrix. The question of the nature of the modes that arise in the ring cannot be solved without studying how excitation is affected by changes in the structure of connections, primarily by turning off and interrupting some of them.

The first question that was stated was: what will happen if after the impact all connections are broken (zero g_{syn})? It is especially important to understand this in the bistable mode, for example, at $g_{\text{L}} = 0.04$. In the example above shown in Fig. 6, *a* it is shown (time series immediately after the impact) that during a time of 100 ms of impact, 7 neurons manage to be sequentially excited, after which the impact was turned off, as and connections between them. It can be seen that in this case the remaining three neurons are not excited, and the excited neurons switched to the mode of their own oscillations, which, due to the difference in the g_{L} parameter from the starting neuron (indicated in black), has a different, lower frequency (see Fig. 3, *b*). This is clearly visible in Fig. 6, *a* below (row after a long transition process), where the black impulse of the zero neuron ($g_{\text{L}} = 0.35$) first follows the purple impulse of the seventh neuron, and then overtakes it (in the middle of the graph at $t \approx 9.9$ ms).

If not all the connections are broken when the external driving is terminated, but only one (between the 4-th and 5-th neurons in Fig. 6, *b*), the ring turns into a chain. Therefore, the neurons excited by external influences manage to bring the remaining ones into an oscillatory mode. As a result, a train of impulses is formed, where the first neuron is the one in front of which the connection was broken, and the last is its neighbor, after which the connection was broken. In this case, the oscillation frequency itself is still inherited from the limit cycle of an individual neuron, but the connection in the chain leads to phase synchronization with a fixed shift due to inertia in the synapse. If the connection between neurons was initially broken (see Fig. 6, *c*), only part of the chain before the break will be excited, but all excited neurons will still be grouped with exactly the same delay as in Fig. 6, *b*.

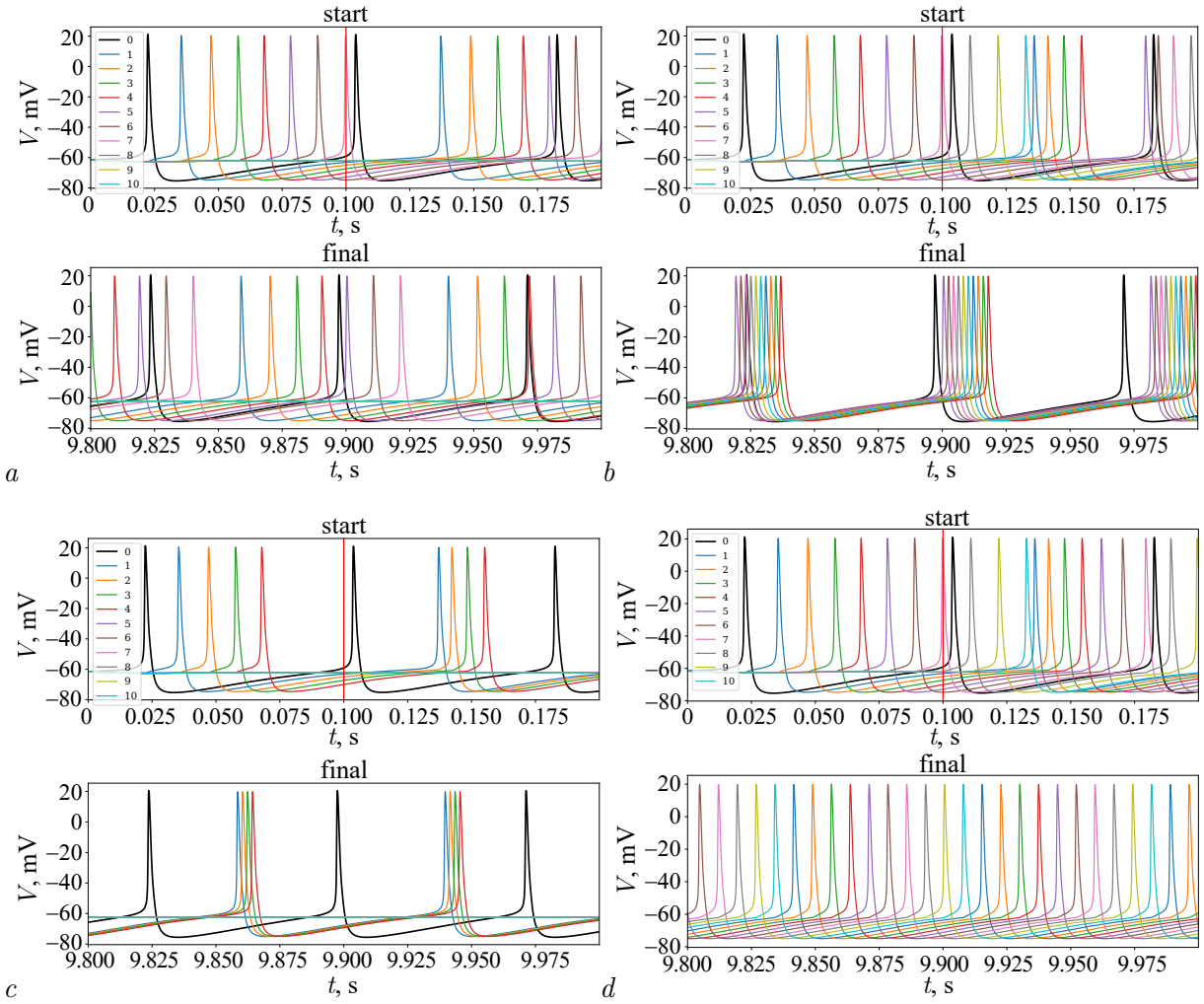

Fig 6. Time series of oscillations in a ring of 10 neurons immediately after the excitation of oscillations (upper figure in each fragment) and after 10 seconds (steady-state mode — lower figure in each fragment) (color online)

Finally, if all connections in the ring are preserved, the oscillation frequency depends both on the own parameters of an individual neuron and on the number of neurons in the ring. This is clearly seen in Fig. 6, *d*. First, immediately after excitation, the time distance between the spikes of neighboring neurons is greater than in the stable regime. This is due to the time shift between the tenth and first neurons turns out to be too small, which leads to further adjustment of the oscillations.

2.4. Network with detuned parameters. To understand the limits of stability of the oscillatory modes detected in the ring, a small detuning was introduced for all parameters except C (an arbitrary change in this parameter is impossible, since it actually leads to a renormalization of time in the first equation of the system (1)), g_{L} (the value $g_{\mathrm{L}} = 0.043$ μS was always used) and $V_0 = 0$. The parameter spread was about 2% in absolute value for each parameter independently. The detuning was introduced randomly. In fact, it is not clear how close this spread corresponds to the distribution of real brain cells. The main results on the study of the parameter spread for hippocampal neurons, including field CA3, are known primarily for morphological rather than electrophysiological parameters, see [18]. Nevertheless, the introduction of detuning is important

for understanding whether the observed regimes are degenerate.

Parameter values for the detuned neurons were generated randomly in a given range of ±2% for each of the parameters g_{Na}, g_{Ca}, $g_{Ca(low)}$, $g_{K(DR)}$, $g_{K(A)}$, $g_{K(AHP)}$, $g_{K(C)}$, V_{Na}, V_{Ca}, V_K, V_{syn}, V_L, ϕ and β_χ. A total number of 600 parameter sets was generated. Of these, two nonoverlapping sets of 35 neurons were selected. The neurons from the first set demonstrated a bistable mode despite the fact that the initial value of $g_L = 0.043$ μS corresponded to a mode with one attractor. The neurons from the second set demonstrated an excitable mode with a single attractor in the form of a stable focus. For both of them, the dependences of the generation frequency f on the number of neurons in the ring D were plotted for different values of synaptic conductivity g_{syn} by analogy with Fig. 4 — see Fig. 7.

A comparison of Fig. 4, *a* and Fig. 7, *a* allows us to conclude that for the case of neurons that were in the bistable mode, the introduction of a detuning in parameters does not affect the dynamics qualitatively: there is still a minimal value of the number of neurons, in this case $D = 8$, at which quasi-synchronous oscillations are destroyed. For the larger D the frequency depends on the number of elements in the network approximately according to a hyperbola with jumps, due to the fact that the total frequency range should be within 13–14.7 Hz. For excitable neurons (see Fig. 4, *b*) the dependence looks more complicated. No sharp drop in frequency, as in Fig. 4, *b* for $g_{syn} = 2.5$, is observed for the detuned neurons. At the same time, if g_{syn} is decreased from $g_{syn} = 2.5$ to $2.2 \leqslant g_{syn} \leqslant 2.4$ μS at relatively large D ($D \geqslant 24$ for g_{syn} $hm = 2.2$ μS and $D \geqslant 27$ for $g_{syn} = 2.4$ μS) there is a sharp drop in frequency to 2 Hz or less. The same drop was seen for identical neurons, but with somewhat larger synaptic conductivity. This behavior of the dependence $f(D)$ for different g_{syn} indicates that the non-identity of neurons leads to a decrease of the region in which the desired mode exists, so to achieve it becomes necessary to reduce the synaptic conductivity (in other terms, the coupling strength). Nevertheless, the mode of slow oscillations, the frequency of which is determined solely by the number of oscillators in the network and the conductivity of the connection and has no relation to the frequencies of the autonomous oscillations of the neuron, turns out to be structurally stable even at the simultaneous variation of 14 parameters. This allows us to hope that a sharp switch in the oscillation frequency in the ring of hippocampal neurons, which occurs with a relatively small change in synaptic conductivity (in our case, between values of 2.4 μS and 2.5 μS) is physiological

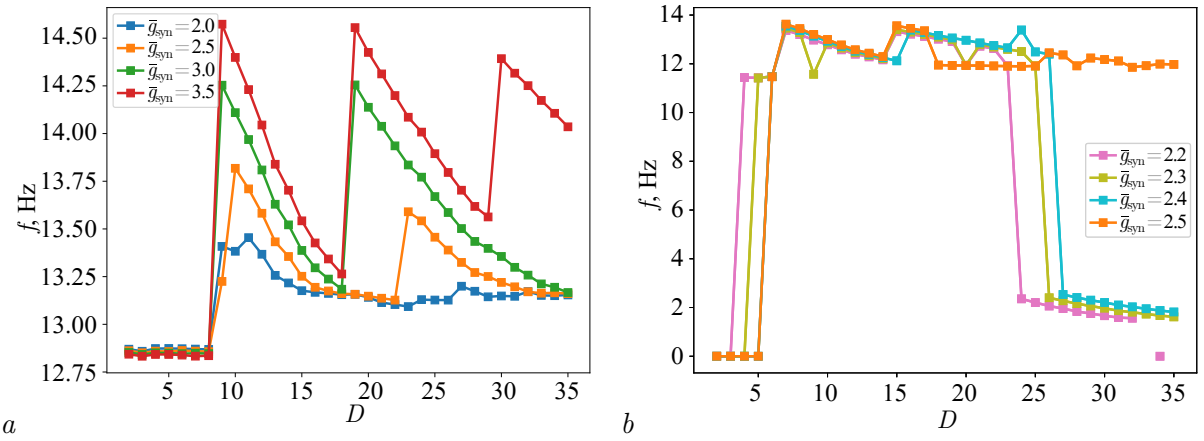

Fig 7. The dependence of the oscillation frequency in the ring f on the number of neurons in the network D at different values of synaptic conductivity g_{syn}. $w = 100$ ms. Leakage conductivity: $g_L = 0.043$ μS. Subplot (*a*) was constructed for the ring composed from bistable neurons, subplot (*b*) was constructed for the ring of excitable neurons (the only attractor in the form of stable focus was available) (color online)

and can indeed determine the transitions between different stages of limbic epileptic discharge.

Conclusion

Mathematical modeling of brain signals at the limbic (temporal lobe) epilepsy is a difficult task, primarily because these signals themselves can be very different. The best known results were obtained using a macroscopic approach, when epileptic activity is described as a whole, and individual neurons are not modeled, see e. g. [19]. Despite the fact that the time series obtained in the work [19] correspond quite well to various types of epileptiform activity during focal seizures, this approach is still rather phenomenological. It ignores the main cause of focal epilepsy — the presence of small neural ensembles (circuits), having a specific pathological structure [20]. There are separate attempts to consider limbic epilepsy from the point of view of mesoscale models [21], including those implementation of possible behavior control (prevention or termination of discharges) [22]. However, the results achieved up to date are highly preliminary, mostly due to the complexity of the phenomenon being modeled and the variety of types of activity in limbic epilepsy.

In this work, we follow our previously proposed approach [8, 10] — breaking the entire modeling process into parts. First of all, we need to model the epileptic focus, which in most cases is located in the hippocampus [23]. This can be a very small network of literally ten of dozen of neurons. Its only function is to generate the basic rhythm of pathological activity. Moreover, the presence and prevalence of long-distance connections in the hippocampus, including in its CA3 formation [24], suggests that such a circuit may not form in any specific place, but may be partially distributed throughout the hippocampus. This corresponds to the ideas about reoccurrence of epilepsy after removal of the epileptic focus [25].

Previously, in the works [8, 10] we proposed a relatively simple mathematical model of the fundamental frequency generator of epileptiform activity, which is a ring of neurons with unidirectional couplings. Numerical and electronic simulations have shown that such a generator can effectively adjust its frequency depending on the number of elements in the ring and the delay time in the connections. In this case, relatively simple FitzHugh–Nagumo equations in [10] or Hodgkin–Huxley equations in their original form in [8] were used as models of individual neurons. These models do not reflect the specifics of hippocampal neurons. In mesoscale modeling, the properties of individual neurons are not so important and the determining factor is the network structure, since each node in the network in reality represents a large number of nodes with similar parameters [26, 27]. On the contrary, in the case of modeling an epileptic focus in the hippocampus, we are actually dealing with microscale modeling, that is, with a ratio of the number of model and real neurons close to 1:1. With this relationship, the choice of model for an individual neuron becomes a key factor. Therefore, in this work, the goal was to determine which properties of the previously proposed ring structure can be effectively repeated using models that reproduce all the main currents in the pyramids of the CA3 field of the hippocampus. One of the key features of such modeling is the refusal to explicitly take into account the delay in the synapse and the transition to equations for the synaptic variable, where the role of the delay is played by inertia.

For network dynamics to be determined primarily by the number of elements in the ring and communication parameters, individual neurons must be in an excitable mode. Otherwise, the natural generation frequency of an individual neuron will greatly limit the frequency tuning capabilities of a ring oscillator. Therefore, a bifurcation analysis was carried out for an individual neuron using the leakage conductivity parameter g_{L}. This analysis showed that during the

transition from the oscillatory mode to the excitable one, two bifurcations occur. First, the subcritical Andronov–Hopf bifurcation, as a result of which a cycle is born from the unstable focus, and the focus itself becomes stable. So, bistability and threshold oscillation excitation of are observed in the system. Second, there is a bifurcation, at which the stable and the unstable cycles merge, as a result of which the stable focus remains the only attractor.

A numerical study of the dependence of the oscillation frequency in the ring on the number of neurons in it in a bistable mode showed that the frequency can vary in a relatively narrow range of 12.7–14.8 Hz. This is due to the existence of an oscillatory attractor for an individual neuron. This mode remains stable even when the ring neurons are detuned in parameters by an amount of about 2% of their absolute value. However, this behavior may be interesting only for modeling a relatively smooth change in frequency at some stages of an epileptic seizure. More interesting is the regime achieved at certain values of synaptic conductivity for models when an individual neuron has a single fixed point attractor. It is characterized by a sharp drop in frequency with an increase in the number of elements in the ring above a certain level. So, the frequency of 2 Hz and lower, characteristic of the depression phase after a discharge in biological experiment, can be achieved. In this oscillation mode, the period actually depends almost linearly on the number of neurons, as was the case in the models proposed earlier in [8, 10]. It becomes clear that the change in synaptic conductivity g_{syn} is the most promising mechanism for variation in oscillation frequency from a physiological point of view rather than a change in the number of neurons in the ring or the delay time in the synapse. This mechanism can lead to both a sharp a drop or increase in the generation frequency several times (for example, from 14 Hz to 2 Hz), and the death of oscillations (which may correspond to the cessation of the discharge) with a further drop in g_{syn}.

References

1. Scheffer IE, Berkovic S, Capovilla G, Connolly MB, French J, Guilhoto L, Hirsch E, Jain S, Mathern GW, Moshé SL, Nordli DR, Perucca E, Tomson T, Wiebe S, Zhang Y-H, Zuberi SM. ILAE classification of the epilepsies: Position paper of the ILAE Commission for Classification and Terminology. Epilepsia. 2017;58(4):512–521. DOI: 10.1111/epi.13709.
2. Suffczynski P, Kalitzin S, Lopes Da Silva FH. Dynamics of non-convulsive epileptic phenomena modeled by a bistable neuronal network. Neuroscience. 2004;126(2):467–484. DOI: 10.1016/j.neuroscience.2004.03.014.
3. Medvedeva TM, Sysoeva MV, Lüttjohann A, van Luijtelaar G, Sysoev IV. Dynamical mesoscale model of absence seizures in genetic models. PLoS ONE. 2020;15(9):e239125. DOI: 10.1371/journal.pone.0239125.
4. Kapustnikov AA, Sysoeva MV, Sysoev IV. Transient dynamics in a class of mathematical models of epileptic seizures. Communications in Nonlinear Science and Numerical Simulation. 2022;109:106284. DOI: 10.1016/j.cnsns.2022.106284.
5. Taylor PN, Wang Y, Goodfellow M, Dauwels J, Moeller F, Stephani U, Baier G. A computational study of stimulus driven epileptic seizure abatement. PLoS ONE. 2014;9(12): e114316.DOI: 10.1371/journal.pone.0114316.
6. Bertram EH. The functional anatomy of spontaneous seizures in a rat model of chronic limbic epilepsy. Epilepsia. 1997;38(1):95–105. DOI: 10.1111/j.1528-1157.1997.tb01083.x.
7. Blumenfeld H, Varghese GI, Purcaro MJ, Motelow JE, Enev M, McNally KA, Levin AR, Hirsch LJ, Tikofsky R, Zubal IG, Paige AL, Spencer SS. Cortical and subcortical networks in human secondarily generalized tonic-clonic seizures. Brain. 2009;132(4):999–1012. DOI: 10.1093/brain/awp028.
8. Kornilov MV, Sysoev IV. Mathematical model of a main rhythm in limbic seizures. Mathe-

matics. 2023;11(5):1233. DOI: 10.3390/math11051233.
9. Mysin IE, Kitchigina VF, Kazanovich YB. Phase relations of theta oscillations in a computer model of the hippocampal CA1 field: Key role of Schaffer collaterals. Neural Networks. 2019;116:119–138. DOI: 10.1016/j.neunet.2019.04.004.
10. Egorov NM, Sysoeva MV, Ponomarenko VI, Kornilov MV, Sysoev IV. Ring generator of neuron-like activity with tunable frequency. Izvestiya VUZ. Applied Nonlinear Dynamics. 2023;31(1):103–120. DOI: 10.18500/0869-6632-003025.
11. Hodgkin A, Huxley A. A quantitative description of membrane current and its application to conduction and excitation in nerve. The Journal of Physiology. 1952;117(4):500–544. DOI: 10.1113/jphysiol.1952.sp004764.
12. Tateno K, Hayashi H, Ishizuka S. Complexity of spatiotemporal activity of a neural network model which depends on the degree of synchronization. Neural Network. 1998;11(6):985–1003. DOI: 10.1016/s0893-6080(98)00086-0.
13. Yoshida M, Hayashi H. Emergence of sequence sensitivity in a hippocampal CA3–CA1 model. Neural Networks. 2007;20(6):653–667. DOI: 10.1016/j.neunet.2007.05.003.
14. Virtanen P, Gommers R, Oliphant TE, Haberland M, Reddy T, Cournapeau D, Burovski E, Peterson P, Weckesser W, Bright J, van der Walt SJ. SciPy 1.0: fundamental algorithms for scientific computing in Python. Nature methods. 2020;17(3):261–272. DOI: 10.1038/s41592-019-0686-2.
15. Pikovsky A, Rosenblum M, Kurths J. Synchronization: A Universal Concept in Nonlinear Sciences. Cambridge University Press; 2001. 411 p. DOI: 10.1017/CBO9780511755743.
16. Senhadji L, Wendling F. Epileptic transient detection: wavelets and time-frequency approaches. Neurophysiologie Clinique/Clinical Neurophysiology. 2002;32(3):175–192. DOI: 10.1016/S0987-7053(02)00304-0.
17. Sobayo T, Fine AS, Gunnar E, Kazlauskas C, Nicholls D, Mogul DJ. Synchrony Dynamics Across Brain Structures in Limbic Epilepsy Vary Between Initiation and Termination Phases of Seizures. IEEE Transactions on Biomedical Engineering. 2013;60(3):821–829. DOI: 10.1109/TBME.2012.2189113.
18. Scorcioni R, Lazarewicz MT, Ascoli GA. Quantitative morphometry of hippocampal pyramidal cells: differences between anatomical classes and reconstructing laboratories. Journal of Comparative Neurology. 2004;473(2):177–193. DOI: 10.1002/cne.20067.
19. Wendling F, Bartolomei F, Bellanger JJ, Chauvel P. Epileptic fast activity can be explained by a model of impaired GABAergic dendritic inhibition. European Journal of Neuroscience. 2002;15(9):1499–1508. DOI: 10.1046/j.1460-9568.2002.01985.x.
20. Paz JT; Huguenard JR. Microcircuits and their interactions in epilepsy: Is the focus out of focus? Nature Neuroscience. 2015;18:351–359. DOI: 10.1038/nn.3950.
21. Myers MH, Kozma R. Mesoscopic neuron population modeling of normal/epileptic brain dynamics. Cognitive neurodynamics. 2018;12:211–223. DOI: 10.1007/s11571-017-9468-7.
22. Alexander A, Maroso M, Soltesz I. Organization and control of epileptic circuits in temporal lobe epilepsy. Progress in brain research. 2016. Vol. 226. P. 127–154. DOI: 10.1016/bs.pbr.2016.04.007.
23. Toyoda I, Bower MR, Leyva F, Buckmaster PS. Early activation of ventral hippocampus and subiculum during spontaneous seizures in a rat model of temporal lobe epilepsy. Journal of Neuroscience. 2013;33(27):11100–11115. DOI: 10.1523/JNEUROSCI.0472-13.2013.
24. Muller RU, Stead M, Pach J. The hippocampus as a cognitive graph. The Journal of general physiology. 1996;107(6):663–694. DOI: 10.1085/jgp.107.6.663.
25. Petrik S, San Antonio-Arce V, Steinhoff BJ, Syrbe S, Bast T, Scheiwe C, Brandt A, Beck J, Schulze-Bonhage A. Epilepsy surgery: Late seizure recurrence after initial complete seizure

freedom. Epilepsia. 2021;62(5):1092–1104. DOI: 10.1111/epi.16893.
26. Medvedeva TM, Sysoeva MV, van Luijtelaar G, Sysoev IV. Modeling spike-wave discharges by a complex network of neuronal oscillators. Neural Networks. 2018;98:271–282. DOI: 10.1016/j.neunet.2017.12.002.
27. Gerster M, Berner R, Sawicki J, Zakharova A, Hlinka J, Lehnertz K, Schöll E. FitzHugh–Nagumo oscillators on complex networks mimic epileptic-seizure-related synchronization phenomena. Chaos. 2020;30:123130. DOI: 10.1063/5.0021420.